



HAL
open science

Septoplasty by disarticulation

R. Jankowski, P. Gallet, D.-T. Nguyen, C. Rumeau

► **To cite this version:**

R. Jankowski, P. Gallet, D.-T. Nguyen, C. Rumeau. Septoplasty by disarticulation. European Annals of Otorhinolaryngology, Head and Neck Diseases, 2020, 137 (5), pp.423-426. 10.1016/j.anorl.2020.07.014 . hal-03492978

HAL Id: hal-03492978

<https://hal.science/hal-03492978v1>

Submitted on 17 Oct 2022

HAL is a multi-disciplinary open access archive for the deposit and dissemination of scientific research documents, whether they are published or not. The documents may come from teaching and research institutions in France or abroad, or from public or private research centers.

L'archive ouverte pluridisciplinaire **HAL**, est destinée au dépôt et à la diffusion de documents scientifiques de niveau recherche, publiés ou non, émanant des établissements d'enseignement et de recherche français ou étrangers, des laboratoires publics ou privés.



Distributed under a Creative Commons Attribution - NonCommercial 4.0 International License

1 Sex chromosome degeneration by 2 regulatory evolution

3
4 Thomas Lenormand^{1,2,*}, Fredric Fyon¹, Eric Sun², Denis Roze^{3,4}

5 1 CEFÉ, Univ Montpellier, CNRS, Univ Paul Valéry Montpellier 3, EPHE, IRD, Montpellier, 34293
6 France

7 2 Radcliffe Institute, Harvard University, Cambridge, MA 02138, USA

8 3 CNRS, UMI 3614, Roscoff, 29680 France

9 4 Sorbonne Université, Station Biologique de Roscoff, France

10 * Correspondence and lead contact: thomas.lenormand@cefe.cnrs.fr

11 Keywords: sex chromosome; population genetics theory; *cis*-regulators; degeneration; selective
12 interference; dosage compensation

13 Summary

14 In many species, the Y (or W) sex chromosome is degenerate. Current theory proposes that this
15 degeneration follows the arrest of recombination and results from the accumulation of
16 deleterious mutations due to selective interference--the inefficacy of natural selection on non-
17 recombining genomic regions. This theory requires very few assumptions, but does not robustly
18 predict fast erosion of the Y (or W) in large populations or the stepwise degeneration of several
19 small non-recombining strata. We propose a new mechanism for Y/W erosion that works over
20 faster timescales, in large populations, and for small non-recombining regions (down to a single
21 sex-linked gene). The mechanism is based on the instability and divergence of *cis*-regulatory
22 sequences in non-recombining genome regions, which become selectively haploidized to mask
23 deleterious mutations on coding sequences. This haploidization is asymmetric, because *cis*-
24 regulators on the X cannot be silenced (otherwise there would be no expression in females).
25 This process causes rapid Y/W degeneration and simultaneous evolution of dosage

26 compensation, provided that autosomal *trans*-regulatory sequences with sex-limited effects are
27 available to compensate for *cis*-regulatory divergence. Although this “degeneration by
28 regulatory evolution” does not require selective interference, both processes may act in concert
29 to further accelerate Y degeneration.

30 Results and Discussions

31 The contemporary theory for the evolution of sex chromosome crystallized in the 1970s
32 [1–3] and applies to both XX/XY and ZZ/ZW sex determination systems, which share important
33 convergent similarities [4]. Both cases involve a chromosome that is heterozygous (the Y or W)
34 and present in only one sex. Although a broad range of situations has been described, in many
35 cases, most of the chromosome has stopped recombining and has degenerated considerably.
36 Current theory, which we term “Degeneration by selective interference” (DSI) has been
37 substantially refined since the 70s’, but its core idea--degeneration caused by selective
38 interference--has remained unchanged [3,5–8]. The theory about selective interference, as well
39 as its empirical evaluation, has also been largely developed since the 70s’, well beyond the case
40 of Y degeneration [9–11]. DSI involves a sequence of steps that occur after the arrest of
41 recombination between the Y and X chromosomes (all our arguments also apply to Z/W
42 chromosome system): (a) degeneration of Y-linked genes by 'selective interference' (also known
43 as the 'Hill-Robertson effect'), due to processes such as Muller's Ratchet, hitchhiking, and
44 background selection [8], (b) facultatively, adaptive silencing of Y-linked genes, and (c) evolution
45 of dosage compensation. A variant of this theory proposes that the accumulation of deleterious
46 alleles in regulatory sequences by selective interference leads to reduced Y gene expression
47 [12]. Y-linked alleles, being partially hidden would then further accumulate deleterious
48 mutations and degenerate [13].

49 In this paper, we propose a new “Degeneration by Regulatory Evolution” (DRE) theory to
50 explain Y chromosome degeneration. The main differences from the DSI model are that our
51 theory does not require selective interference, and that steps a-c occur simultaneously after
52 recombination suppression. We previously showed that, for autosomal genes, a ‘*cis*-regulator
53 runaway’ process occurs that leads stronger *cis*-regulators to become associated with

54 chromosomes with fewer deleterious mutations [14]. This favors the stronger *cis*-regulatory
55 alleles, provided they are tightly linked to their coding gene. We also showed that *cis*-regulators
56 diverge in asexuals, where diploid expression is unstable and quickly becomes “haploidized”
57 [15]. DRE theory involves such divergence of *cis*-regulators, but with an asymmetry between the
58 X and Y chromosomes (preventing the suppression of gene expression on the X). We investigate
59 DRE using individual-based stochastic simulations of a population of N_{pop} diploid individuals,
60 with XY males and XX females. In order to capture the essence of the mechanism, we first study
61 a minimal system with only four loci (Figure 1): a gene G , its *cis*-regulator C , and two *trans*-
62 regulators T (we will then extend the model to the case of a non-recombining region comprising
63 a larger number of genes). *Trans*-regulators, such as transcription factors, are not closely linked
64 to their target gene, and influence expression on both homologs, whereas *cis*-regulators, such
65 as enhancers, control the expression of the closely linked gene, and influence only the copy
66 carried on the same chromosome as themselves [16]. We assume that G and C are present on
67 both sex chromosomes, and that they recombine (in females only) at a rate R_c . We include
68 *trans*-regulators in order to examine whether, and over what time-scale, dosage compensation
69 will evolve when expression of the Y-linked allele decreases. With these *trans*-regulators, overall
70 expression can be maintained, i.e. dosage compensated, even if *cis*-regulators change and
71 diverge between the X and Y. Dosage compensation cannot evolve if the *trans*-regulators act in
72 the same way in both males and females, or equally on the X and the Y. Hence we do not
73 consider all potential *trans*-regulators, but only those that could influence dosage
74 compensation. Specifically, we focus on the simplest symmetrical case with one *trans*-regulator
75 expressed in males T_m , and one in females T_f . Both cases have been described empirically (*C.*
76 *elegans* dosage compensation works by halving X expression in females, whereas in *Drosophila*,
77 it works by doubling X expression in males [17]). For simplicity, we assume that these T loci are
78 autosomal and that they recombine freely with each other and with the G and C loci.

79 This initial model is later extended to $n_L CGT_m T_f$ quadruplets of genes (where $n_L = 1, 50,$
80 500). In these models, we assume that the C and G loci are uniformly spaced on the sex
81 chromosomes, with two adjacent genes G recombining at a rate R_g in females, and where each
82 C locus is assumed to be closer to the G gene it regulates than to the next G gene (ten times

83 closer in the simulations,); again, recombination is assumed not to occur in males, representing
84 a non-recombining region including the sex-determining locus, while all T factors are again
85 assumed to recombine freely with the sex-determining region. In this model, each CG pair is
86 influenced by its own $T_m T_f$ pair, which represents the lowest degree of pleiotropy of these *trans*-
87 acting factors, but involves a very high number of *trans*-regulators. We also considered a model
88 where only one $T_m T_f$ pair controls all the G and C loci, representing the other extreme case
89 where *trans*-regulators are maximally pleiotropic and influence many (here all n_L) genes.

90 Deleterious mutations occur within genes G at a rate U_G per gene. Their fitness effect s is
91 drawn from an exponential distribution with mean s_{mean} . The effects of multiple mutations in
92 the same gene are assumed to be additive, but with a maximum effect per gene, s_{max} (which
93 may be interpreted as the fitness effect of a full gene knock-out). Their dominance depends on
94 the strength of their associated *cis*-regulator (see STAR methods). The effects of alleles at the
95 *cis*- (C) and *trans*-regulators (T_m , T_f) are modelled as quantitative traits denoted by c , t_m , t_f ,
96 respectively, and control the level of expression Q of the gene, which is under stabilizing
97 selection with intensity I (STAR methods). The different events of the life cycle occur in the
98 following order: diploid selection, meiosis with recombination, mutation, and syngamy.
99 Simulations are initialized with no polymorphism present, and the optimal gene expression level
100 (no deleterious allele, all c and t_m , t_f alleles fixed to 1). After a burn-in phase where the
101 chromosome evolves with recombination in both sexes, we stop XY recombination in males to
102 create a sex-linked region and follow the frequencies and effects of deleterious mutations on
103 the X and Y, as well as the evolution of the regulatory genes. These outputs are averaged over
104 different numbers of replicates depending on the variance in the process under different
105 parameter values (STAR methods, Table S1). At regular intervals, we compute $P_{halfsilent}$, the
106 probability (across replicates) that Y allele-specific expression $\phi_{Y,i}$ decreased by two fold from
107 the initial value of 0.5 to $\phi_{Y,i} < 0.25$. A complementary approach to quantify partial silencing is
108 to measure the dominance coefficient of deleterious alleles on the Y, measured by $h_{Y,i} =$
109 $\phi_{Y,i}^{-\ln h / \ln 2}$ (see STAR methods). We also compute P_{silent} , the probability that $\phi_{Y,i}$ becomes
110 close to zero (below 0.01), so that alleles on the Y become nearly entirely recessive. The
111 quantity $P_{halfdead}$ then refers to the probability that, by a given number of generations after the

112 Y-linked region stopped recombining, deleterious mutations on the Y gene copy have reduced
113 fitness by an amount $s_{max}/2$, and P_{dead} that they reduced fitness by an amount s_{max} , indicating
114 that the gene has entirely degenerated on the Y.

115 Figure 2 illustrates the process with $n_L=1$ (one gene, one *cis*-regulator, one male limited and one
116 female limited *trans*-regulator). The system does not generate any male-female or X-Y
117 asymmetry before recombination arrest (STAR methods, Figure S1). After recombination arrest,
118 the gene carried by the Y degenerates: it becomes progressively recessive, as h_Y changes from h
119 $= 0.25$ to zero, and accumulates deleterious mutations (the overall fitness effect of mutations
120 present on the Y copy increases up to s_{max}), despite there being very limited selective
121 interference (at most only occurring between the gene and its *cis*-regulator). Silencing occurs
122 first, and the accumulation of deleterious mutations follows later in the process (the curve
123 representing $P_{halfsilent}$ is ahead of the one showing the accumulation of deleterious mutation on
124 the Y, as measured by $P_{halfdead}$). Degeneration also occurs with full dosage compensation, and
125 overall expression never departs from the optimum in either sex (Figure 2B). Compensation
126 typically involves, at least initially, a mixture of upregulation of X gene copies in males and
127 downregulation in females (STAR methods, Figure S3).

128 What is the underlying cause of this asymmetrical degeneration? Once X and Y stop
129 recombining, diploid expression becomes unstable. *Cis*-regulators on the X and Y can diverge,
130 eventually leading to the haploidization of expression in males. This is not prevented by
131 stabilizing selection on expression levels as long as *trans*-regulators can coevolve to maintain
132 near optimal total expression in both sexes. When the strength of *cis*-regulators on the Y starts
133 decreasing, the process is accelerated by a “haploidization” positive feedback loop. Indeed,
134 weak Y *cis*-regulators become associated with coding sequences carrying more deleterious
135 mutations, as they cause a reduction in dominance. They are then selected to weaken further in
136 order to mask those deleterious mutations, which leads to the accumulation of even more
137 deleterious mutations, and so forth. By contrast, the other ‘haploidized’ situation (where the X
138 is silenced in males) is reversible, as X chromosomes with weak *cis*-regulators and a higher load
139 of deleterious mutations cannot fix, as they become homozygous and selected against in
140 females when too frequent (unlike partially silenced Y genes, which can spread as they stay

141 heterozygous in males). Therefore, the regulatory system has only one stable equilibrium,
142 where the Y is silenced and degenerate.

143 Selective interference plays no role in this process, explaining why degeneration occurs even for
144 a single Y-linked gene. However, the process is stochastic, as it is initiated by a random
145 departure from diploid expression with a sufficiently weak Y *cis*-regulator to trigger the
146 “haploidization” feedback loop. In individual simulation replicates, degeneration is indeed very
147 abrupt, but occurs at varying time points (Figure 2A). Because of this stochasticity, the process is
148 slowed down in larger populations: it is ~10 times slower in ~10 times larger populations
149 (Figure 2D). With the same parameters but without mutation in the *cis*-regulator ($U_c = 0$, Figure
150 2C), as in DSI theory, degeneration does not occur, as expected, since there is neither selective
151 interference nor *cis*-regulatory divergence. Degeneration does not occur either in the absence
152 of mutation in the *trans*-regulators ($U_t = 0$, Figure 2C) and for the same parameter values, since
153 *cis* and *trans*-regulators have to coevolve to maintain total expression levels: if *trans*-regulators
154 cannot evolve, the divergence of *cis*-regulators is prevented and Y degeneration cannot occur.
155 However, if the intensity of stabilizing selection on expression levels is weak enough,
156 degeneration evolves but is not dosage compensated (Figure 2C). Otherwise, the intensity of
157 stabilizing selection on dosage only plays a marginal role in DRE (Figure 2C). Control simulations
158 without mutation in the coding gene ($U_G = 0$, Figure 2C) show that *cis*-regulatory divergence and
159 Y silencing can occur even in the absence of deleterious mutations, but as expected, this
160 silencing is slower, not being accelerated by the “haploidization” feedback loop, and reversible
161 (STAR methods, Figure S2).

162 As expected, DRE and DSI combine when more than a single Y-linked gene is considered. The
163 effect is strong: Figure 3 shows that a 50-fold or 500-fold increase in the number of loci results
164 in degeneration being 5-fold and 10-fold faster, respectively: a larger non-recombining Y-linked
165 region degenerates faster than a small one. Without mutation in regulators (i.e. with only DSI),
166 degeneration occurs but is 23-36 fold slower with 50 loci (depending on the control used for the
167 comparison, STAR methods, Figure 4). With 500 loci, however, the comparison with and without
168 regulators is problematic, as very quickly, a modest accumulation of deleterious mutations on
169 the many Y-linked genes causes an important reduction in male average fitness, so that male

170 fitness reaches unrealistically low values (of the order 10^{-17}). Even if a proportion of genes
171 affecting male fitness may be under soft selection, it seems unlikely that a population with such
172 a low male fitness would survive.

173 The drop in male fitness is less dramatic with regulatory evolution, as those mutations become
174 progressively more recessive as the Y degenerates. There is nevertheless a transient drop in
175 male average fitness, which can be quite large (e.g. 3% and 85% reduction for a 50-gene and
176 500-gene Y-linked region, respectively, Figure 3). Data on divergence between sex
177 chromosomes indicate that Y degeneration is often sequential in chiasmate species, with
178 several regions of various sizes, termed “strata” [18], having stopped recombining at different
179 time points. This high transitory fitness drop may prevent large strata from occurring in small
180 populations and may bias towards scenarios involving multiple small strata as, for example, in
181 humans [19]. Comparatively, these scenarios involving small strata are more difficult to explain
182 with DSI, as selective interference is weak on small non-recombining regions.

183 Last, degeneration is initially slower but faster overall when there is only one T_m and T_f
184 controlling all *cis*-regulators. Despite being highly pleiotropically constrained, having only two
185 autosomal *trans*-regulators precipitates degeneration: the tipping point where it is worth fully
186 silencing the Y is quickly reached when many very weakly deleterious mutations have
187 accumulated on the Y. This is consistent with the observation that dosage compensation can
188 occur locally on a gene-by-gene basis or by chromosome-wide *trans*-acting effects [17].
189 Intermediate cases involving *cis*- and *trans*-regulators with regional effects [as e.g. in *Drosophila*
190 20] may be worth investigating, but are likely to behave similarly, as long as *trans*-regulators
191 only target X genes that have a copy on the Y non-recombining region.

192 Simulations for lower values of mutation rates and strength of selection against deleterious
193 alleles are shown on Figure S4 (for $n_L = 1$ and $n_L = 50$, STAR methods). Unsurprisingly, reducing
194 mutation rates slows degeneration, while the effect of s is more complicated. However, the
195 acceleration of degeneration caused by regulatory evolution still holds. Figure S4 also shows
196 that a scaling argument from diffusion theory indicates that larger populations with weaker
197 mutation and selection should also behave similarly, albeit on a longer timescale.

198 The DRE theory proposes a different view of sex-chromosome evolution compared to the DSI
199 theory that has been developed over the past 40 years. In both cases, degeneration starts after
200 the arrest of recombination in a genome region completely linked to the sex-determining locus.
201 In both cases, degeneration is slower in larger populations, but this is considerably less so in the
202 DRE model. However, there are important differences. With very few exceptions [21,22], DSI
203 was developed without explicitly modelling regulatory evolution. With DSI, regulatory evolution
204 (Y silencing and dosage compensation) is supposed to occur only after deleterious mutations
205 have accumulated on the Y [3,23–25], although it has also been proposed that silencing may
206 result directly from the accumulation of deleterious mutations in regulatory regions [13]. This is
207 certainly possible, as selective interference applies to all functional sequences and may
208 contribute to the fixation of many kinds of deleterious mutations, including those maintaining
209 adequate expression levels. DRE is based on a reverse causality: regulatory evolution initiates
210 the degeneration process. Contrary to the standard model where compensation is needed
211 because degeneration damages genes' function in males, compensation evolves here from the
212 very beginning of the process, by reducing the proportion of transcripts from Y-linked relative to
213 X-linked alleles and maintaining an almost constant overall level of expression in both sexes.
214 However, compensation may not occur when expression levels are under weak stabilizing
215 selection (Figure 2C). Whether compensation occurs on a gene-by-gene basis or chromosome
216 wide depends on the availability of the corresponding *trans*-acting factor, but both can occur in
217 DRE, and, surprisingly, at approximately the same rate (Figure 3).

218 The specific mode of dosage compensation depends on the type of *trans*-regulators. Here we
219 considered *trans*-regulators with sex-limited expression, which can mimic several well-known
220 dosage compensation systems (female-limited factors corresponding to *C. elegans* or mammal
221 systems, while male-limited factors would be more similar to a *Drosophila*-like situation [17],
222 STAR methods). The symmetric DRE model that we used often led to a *Drosophila*-like
223 compensation, where the X in males was eventually expressed twice as much compared to the
224 situation at the recombination arrest (Figure 2B). However, this is certainly dependent on the
225 relative mutation rates on the different types of *trans*-regulators. The theory should be

226 extended to examine the diversity of dosage compensation mechanisms, including sex-of-origin
227 effects [26].

228 Overall, we have presented an alternative theory for the degeneration of sex chromosomes.
229 Although many underlying parameters are still poorly known, this theory could be tested
230 quantitatively, as it works faster than current theory, on smaller non-recombining regions, and
231 does not require small population sizes or recurrent beneficial mutations causing hitchhiking
232 effects. It does not exclude selective interference, which will necessarily co-occur as long as
233 many genes stop recombining simultaneously. However, a hallmark of DRE is that regulatory
234 changes occur very early. This is consistent with recent studies showing that dosage
235 compensation evolves early on [27,28] and that Y transcriptional downregulation accompanies
236 degeneration of protein-coding genes from the start [29–31].

237 Acknowledgments

238 We thank G. Marais, B and D. Charlesworth, S. P. Otto and two anonymous reviewers for
239 insightful comments. We thank MBB cluster from Labex CEMEB, Harvard Odyssey cluster and
240 CNRS ABiMs cluster. We thank J Wakeley for helping access Odyssey cluster. TL and DR
241 acknowledge Radcliffe Institute, CNRS, and grant GenAsex ANR-17-CE02-0016-01 for support.

242 Author contributions

243 Original idea TL, FF; Model conception TL, DR, FF; Code DR, TL, ES; Simulations TL, ES; Data
244 analyses TL; Interpretation TL, DR; First draft TL, FF; Editing TL, DR, ES; Reviews TL, DR; Project
245 management and funding TL.

246 Declaration of interest

247 The authors declare no competing interests.

248

249 Figure Legends

250 **Figure 1 Model presentation.** (A) The simplest genetic model involves autosomal *trans*-
251 regulators expressed either in males or females, and a sex-linked *cis*-regulator controlling the
252 expression of a coding gene. A deleterious allele **a** at the coding gene is expressed at the same
253 level as the wild type **A** allele if their associated *cis*-regulators have equal strength. (B) If there is
254 *cis*-regulatory variation, the deleterious allele may be over or under-expressed, depending on
255 whether it is associated with the stronger or weaker *cis*-regulator. This can be considered as
256 determining the dominance of the **a** allele. The black curve shows the fitness of an Aa
257 heterozygote (y-axis) for varying allele-specific expression levels (x-axis). (C) Selection also acts
258 on the total amount of protein produced (x-axis), with stabilizing selection around an optimal
259 amount. The maximal fitness effect of a departure from the optimal amount is s_{max} , the same as
260 the maximal fitness effect of a deleterious mutation in the coding gene.

261 **Figure 2. Y degeneration by regulatory evolution.** (A) x-axis: time in number of generations, in
262 log-scale. Recombination stops between the X and Y chromosome at generation 250000
263 (vertical dashed gray line); y-axis: The probability that a coding gene on the Y is expressed at less
264 than half the level of the X copy (half-silent, light green curve), entirely silenced (dark green
265 curve), has accumulated deleterious mutations reducing fitness effect half as much as a loss-of-
266 function mutation (half-dead, orange curve), or as much as a full loss-of-function mutation
267 (dead, red curve). Curves are averages over 100 replicates of the process. The model was run
268 with $n_L = 1$ (one gene, one *cis*-regulator, one female and one male limited *trans*-regulator).
269 Parameter values are: population size $N = 10^5$; Mutation rates $U_G, U_C = 2 \times 10^{-4}$; $U_T = 10^{-4}$;
270 recombination rate between the gene and the *cis*-regulator $R_C = 5 \times 10^{-5}$ (in both sexes during
271 the burn-in period, and in females thereafter). The mean effect of each deleterious mutation in
272 the coding gene $s_{mean} = 0.05$ (and loss-of-function effect $s_{max} = 0.3$, dashed gray line). The
273 dominance coefficient of deleterious mutations (when both alleles are equally expressed) is $h =$
274 0.25 , and the intensity of stabilizing selection on dosage $l = 0.1$. The figure also shows the
275 dominance of deleterious mutations carried on the Y (h_Y , blue curve) and the average fitness
276 effect of alleles on the Y (s_Y , purple curve). Some individual trajectories are indicated for h_Y and
277 s_Y (same color code, thin lines) to show that degeneration occurs abruptly in each replicate. (B)

278 Time-variation of regulatory traits corresponding to the case illustrated in panel a. x-axis: time in
 279 number of generations (in log-scale); y-axis: regulator trait values. Pink: X *cis*-regulator strength;
 280 Blue: Y *cis*-regulator strength; Brown: *trans*-regulator strength (plain: female limited, dashed:
 281 male-limited). Optimal dosage is 2 (dashed gray line). Total expression in males and females is
 282 indicated by the dotted curves (male value in blue, female in red). Regulatory trait values before
 283 recombination arrest are not stable due to runaway evolution [14], but are rescaled at 1 at
 284 generation 250000 for fair comparisons across parameter values. They are represented at this
 285 rescaled value on the figure, to avoid overloading the figure (see STAR methods and Figure S1-
 286 S3 for further details). **(C)** Values of s_Y , h_Y and P_{dead} at generation 3×10^6 , for simulations like in
 287 panel (a) except for some parameter values. The star indicates weaker stabilizing selection (I
 288 $=0.01$) compared to $I = 0.1$ in panel (a). NOG ($U_G = 0$); REC (no arrest of recombination); NOCT
 289 ($U_C = U_T = 0$); NOT ($U_T = 0$); REG (with mutations on gene and regulators, as in panel a); FREE (R_c
 290 $= 0.5$); SYM (symmetrized stabilizing selection function, see STAR methods). **(D)** Accumulation of
 291 deleterious mutations on the Y for different population sizes (10^3 , 10^4 like in panel a, 10^5). x-
 292 axis: number of generations in log-scale. y-axis: s_Y . Plain lines: with evolving regulators. Dotted
 293 lines: without regulator evolution (NOCT simulations, $U_C = U_T = 0$). Table S1 summarizes the
 294 different simulations, parameter values and number of replicates.

295 **Figure 3 DRE with many loci.** Y degeneration in non-recombining regions with n_L loci. **(A)** $n_L =$
 296 50. **(B)** $n_L = 500$. Coding genes are positioned at regular interval on the X/Y chromosome, each at
 297 a recombination rate $R_G = 5 \times 10^{-4}$ (map length of the non-recombining region is therefore 2.5 or
 298 25 cM, respectively). Recombination occurs in both sexes during the burn-in period (ending at
 299 2.5×10^5 generations, vertical dotted line), and in females thereafter. x-axis: number of
 300 generation in log-scale. y-axis: degeneration of the Y, as measured by P_{dead} , in log-scale (plain
 301 lines) or male mean fitness (dashed lines). Red: the $n_L = 1$ case given for comparison. Dark red:
 302 n_L genes with n_L male-limited *trans*-acting factors and n_L female-limited trans acting factors.
 303 Brown: n_L genes with 1 male-limited *trans*-acting factor and 1 female-limited trans acting factor
 304 influencing all *cis*-regulators. Gray: n_L genes without regulatory evolution (NOCT simulations, U_C
 305 $= U_T = 0$). Other parameters are as in Figure 2A. Note the different time range in panels (a) and
 306 (b). In the absence of regulatory evolution (NOCT simulations), with $n_L = 500$, male average

307 fitness drops quickly to a vanishingly small number (to the order 10^{-17} after a million generation)
308 that should lead to population extinction, as indicated by the skull symbol. This drop occurs
309 quickly, even before any appreciable mutation accumulation on genes (i.e. it is already down to
310 the inverse of population size when s_Y reaches ~ 0.01). Table S1 summarizes the different
311 simulations, parameter values and number of replicates. See also Figure S4.

312 **Figure 4 Comparing DRE and DSI.** Y degeneration in non-recombining regions with 50 loci.
313 Coding genes are positioned at regular interval on the X/Y chromosome, each at a
314 recombination rate $R_G = 5 \times 10^{-4}$ (map length of the non-recombining region is therefore 2.5
315 cM). Recombination occurs in both sexes during the burn-in period (ending at 2.5×10^5
316 generations, vertical dotted line), and in females thereafter. *x*-axis: number of generations in
317 log-scale. *y*-axis: degeneration of the Y, as measured by P_{dead} , in log-scale. **Dark red:** 50 genes,
318 with 50 *cis*-regulators, 50 male-limited *trans*-acting factors and 50 female-limited *trans* acting
319 factors. **Dark red, dashed:** 50 genes, with 50 *cis*-regulators, no mutation in *trans*-regulators
320 (NOT simulations, $U_T = 0$). **Gray, dashed:** 50 genes, with 50 *cis*-regulators, no *trans*-regulators
321 (NOT simulations, $U_T = 0$), but dominance of the effect of mutations on genes maintained at $h =$
322 0.25. **Gray:** 50 genes without regulatory evolution (NOCT simulations, $U_C = U_T = 0$). Other
323 parameters are as in Figure 2A. Table S1 summarizes the different simulations, parameter
324 values and number of replicates. See also Figure S4.

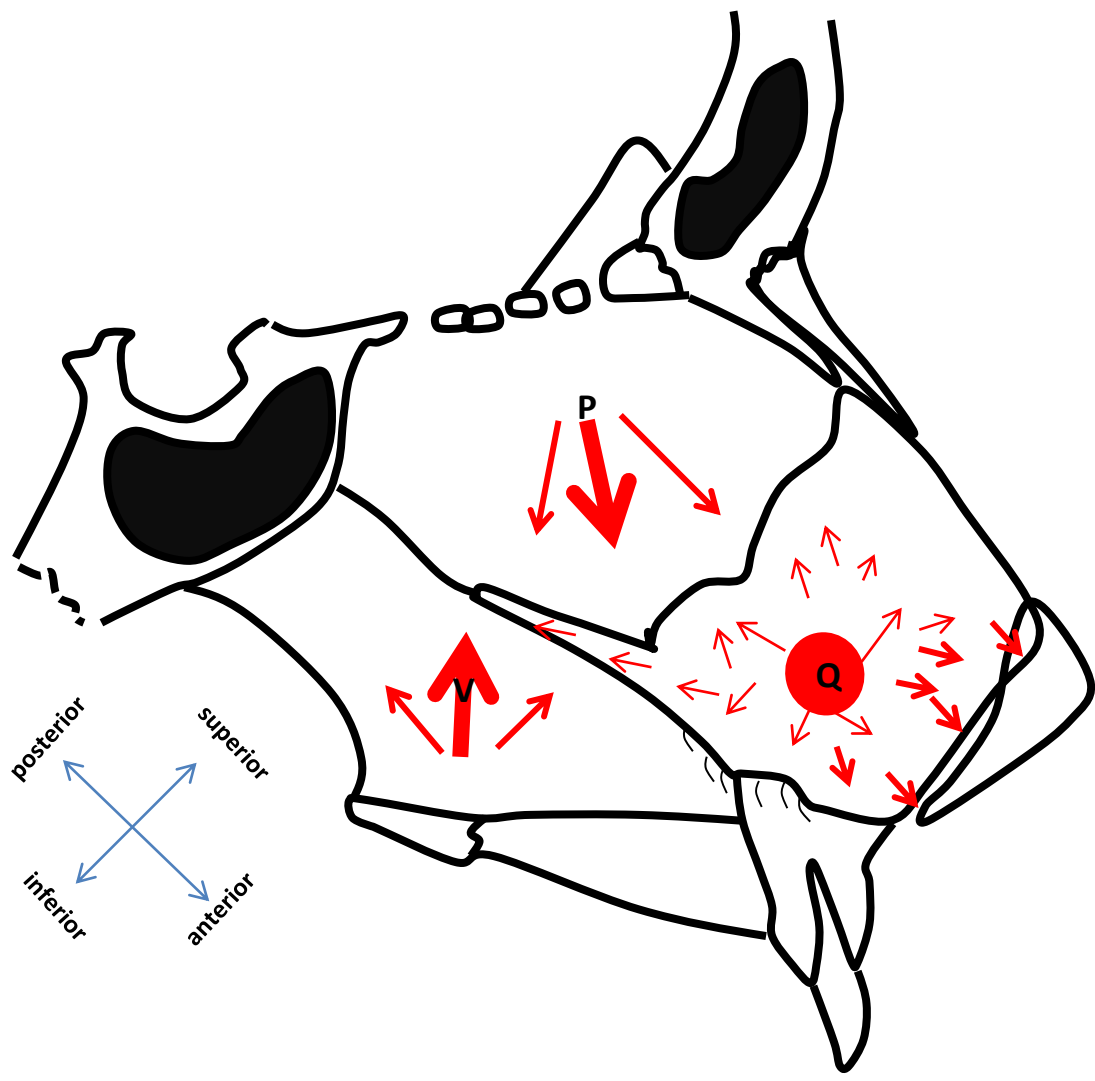
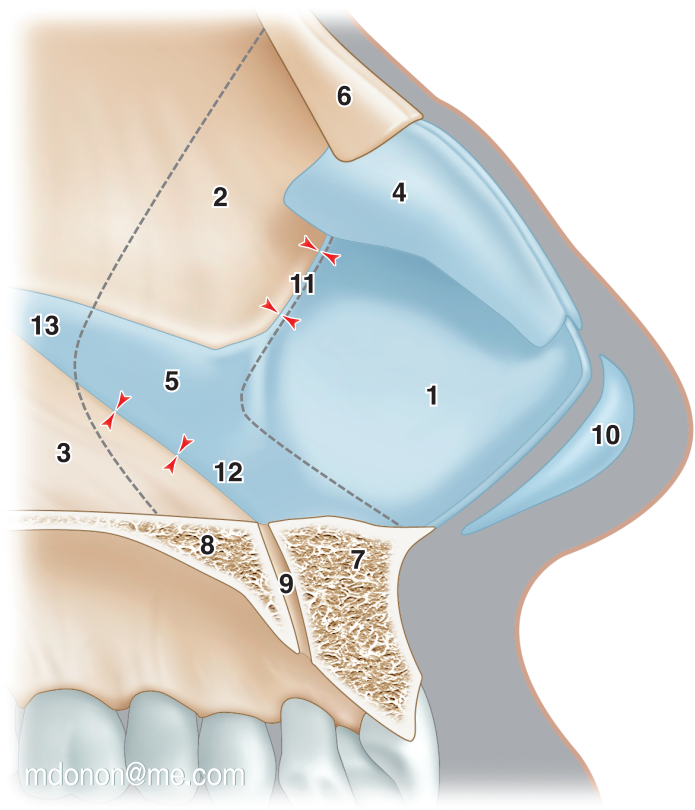
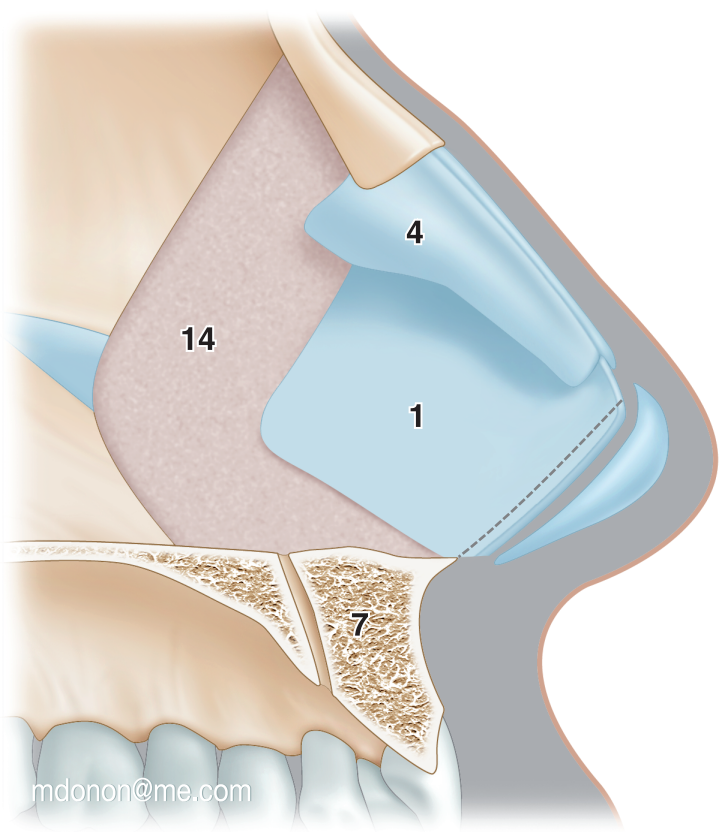


Figure 1



mdonon@me.com



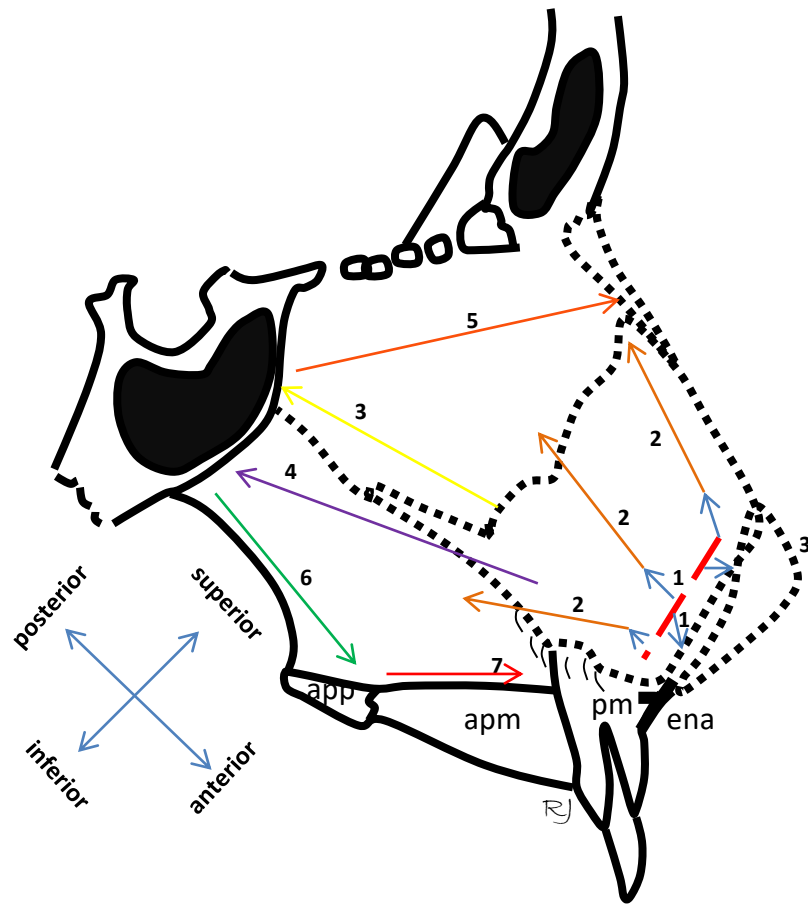


Figure 4

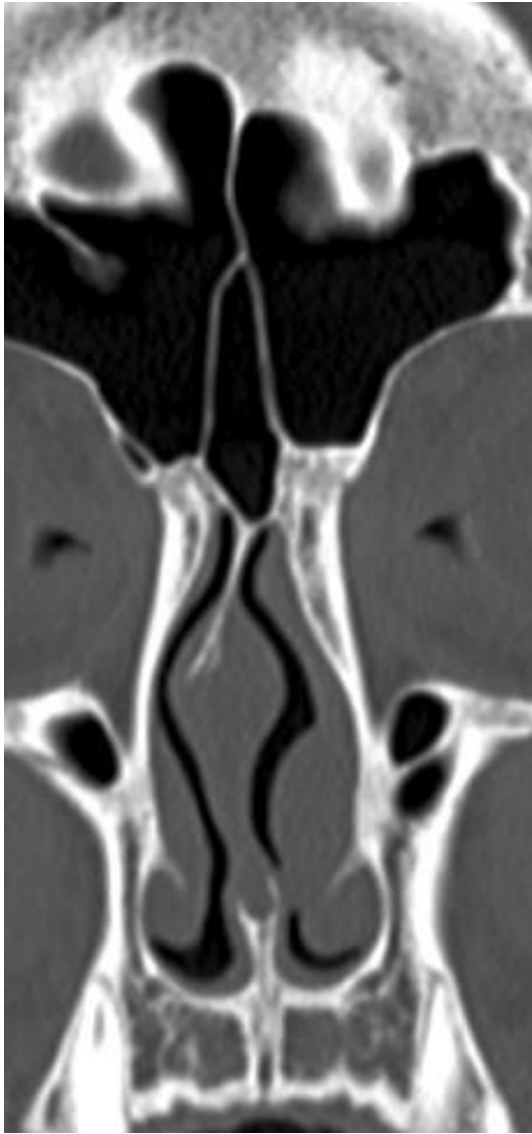


Figure 5: